Int. J. Electrochem. Sci., 8 **(2013)** 3333 - 3348

International Journal of ELECTROCHEMICAL SCIENCE
www.electrochemsci.org

Synthesis, Characterization and Electrochemical Analysis of V-Shaped Disubstituted Thiourea-Chlorophyll Thin Film as Active Layer in Organic Solar Cells

Rafizah Rahamathulla1[1], *Wan M. Khairul*[1*], *Hasiah Salleh*[2], *Hasyiya Karimah Adli*[1], *M.I.N. Isa*[2] *and Meng Guan Tay*[3]

[1]Advanced Materials Research Group, Department of Chemical Sciences, Faculty of Science and Technology, Universiti Malaysia Terengganu, 21030 Kuala Terengganu, Malaysia.
[2]Advanced Materials Research Group, Department of Physical Sciences, Faculty of Science and Technology, Universiti Malaysia Terengganu, 21030 Kuala Terengganu, Terengganu, Malaysia.
[3]Faculty of Resource Science and Technology, Universiti Malaysia Sarawak, 94300 Kota Samarahan, Sarawak, Malaysia.
[*]E-mail: wmkhairul@umt.edu.my

Received: 30 December 2012 / *Accepted:* 28 January 2013 / *Published:* 1 March 2013

Conjugated thiourea system has attracted considerable attention as potential molecular framework to construct molecular components for molecular electronics. To date, thiourea systems are surprisingly unexplored although the well-known rigid π-systems enhance the development of molecular wire architecture to be applied as potential organic solar cell (OSC). Regarding to this matter, a study on the performance of conjugated V-shaped disubstituted thiourea compound systems to act as potential active layer in OSC was carried out prior to form photovoltaic thin film. The compound namely N^1,N^3-bis(4-(octyloxy)phenyl)-*N*-(benzene-1,3-dicarbonyl) thiourea was spectroscopically and analytical characterized via Fourier Transform Infrared (FT-IR), UV-Visible Analysis (UV-Vis), CHNS elemental analysis, ^{1}H and ^{13}C Nuclear Magnetic Resonance (NMR), Thermogravimetric Analysis (TGA), Scanning Electron Microscopy (SEM) as well as Cyclic Voltammetry (CV) analysis. In turn, it was fabricated on Indium Tin Oxide (ITO) substrate before its conductivity behaviour, efficiency and OSC parameter were evaluated by Four Point Probe. From the electrical conductivity study, it revealed that the layer of ITO/V-shaped thiourea thin film exhibits higher conductivity, 0.1377Scm^{-1} with the presence of chlorophyll (CHLO) under maximum light intensity of 100 Wm^{-2}. Therefore, further evaluation of this type of molecular framework featuring thiourea moiety should be taken to enhance the development in the area of microelectronic devices.

Keywords: Organic Solar Cell, Chlorophyll/Thiourea/ITO, molecular wire.

1. INTRODUCTION

Global warming and energy consumption turn out to become major and serious issues recently which affect human and environment [1]. Therefore, rapid action of finding an environmentally safe renewable energy source should be taken tremendously [2].

There is a widespread interest onto the conveniently of using alternative global energy that utilize solar energy due to their simple fabrication process and minimal material usage [3-5]. There were few reports on newly invented solar cell that show a great promise of organic electronic which provide safe environmental, flexible, lightweight and inexpensive electronics [6,7]. Moreover, the preparation of organic thin film has become as an interesting topic as it has opened a new class of materials to be used in various microelectronics such as organic solar cell (OSC), semiconductor and photoconductor.

Undoubtedly, organic materials are attractive for future application in solar cell devices via possibilities in the form of ultra thin and flexible devices which may integrate into appliance or building material [8-10]. For the active elements in organic solar cell, conjugated molecule both posse optical absorption and charge transport are dominated by partly delocalized π and π* orbital [11,12]. Indeed, this behavior plays a crucial role in order to absorb light [13]. Electronic devices that use single organic molecules as active elements have become potentially promising alternatives [14,15].

However, it is a challenging procedure in order to find suitable and applicable ideal molecular materials for its utilization in solar cell devices [16]. Thus, these issues arise in the design and the construction of molecular wires as active layer in organic solar cell [17]. In previous occasion, we have introduced essentially linear conjugated system of the particular molecular framework [18]. However, the reports on the synthesis and properties of conjugated thiourea for single molecule solar cells are rather limited. Therefore, in present study, we introduce and investigate the performances of rigid π-system of V-shaped disubstituted thiourea namely N^1,N^3-bis(4-(octyloxy)phenyl)-*N*-(benzene-1,3-dicarbonyl) thiourea as shown in Figure 1. The difference in alkoxy chain length on the substituted thioureas is expanded and elongated which are expected to lead to even more interesting active layer properties. Moreover, this study focuses on the arrangement of organic thin films by layering with chlorophyll that doped on the conjugated thiourea (TU) to increase the ability of light absorption.

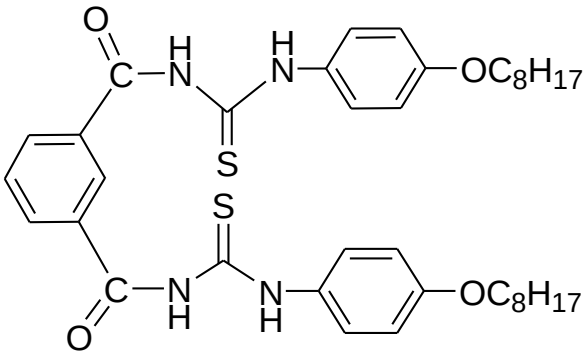

Figure 1. Molecular structure of N^1,N^3-bis(4-(octyloxy)phenyl)-*N*-(benzene-1,3-dicarbonyl) thiourea (**3**) as active layer in organic solar cell.

2. EXPERIMENTAL

2.1. Material and General Methodology

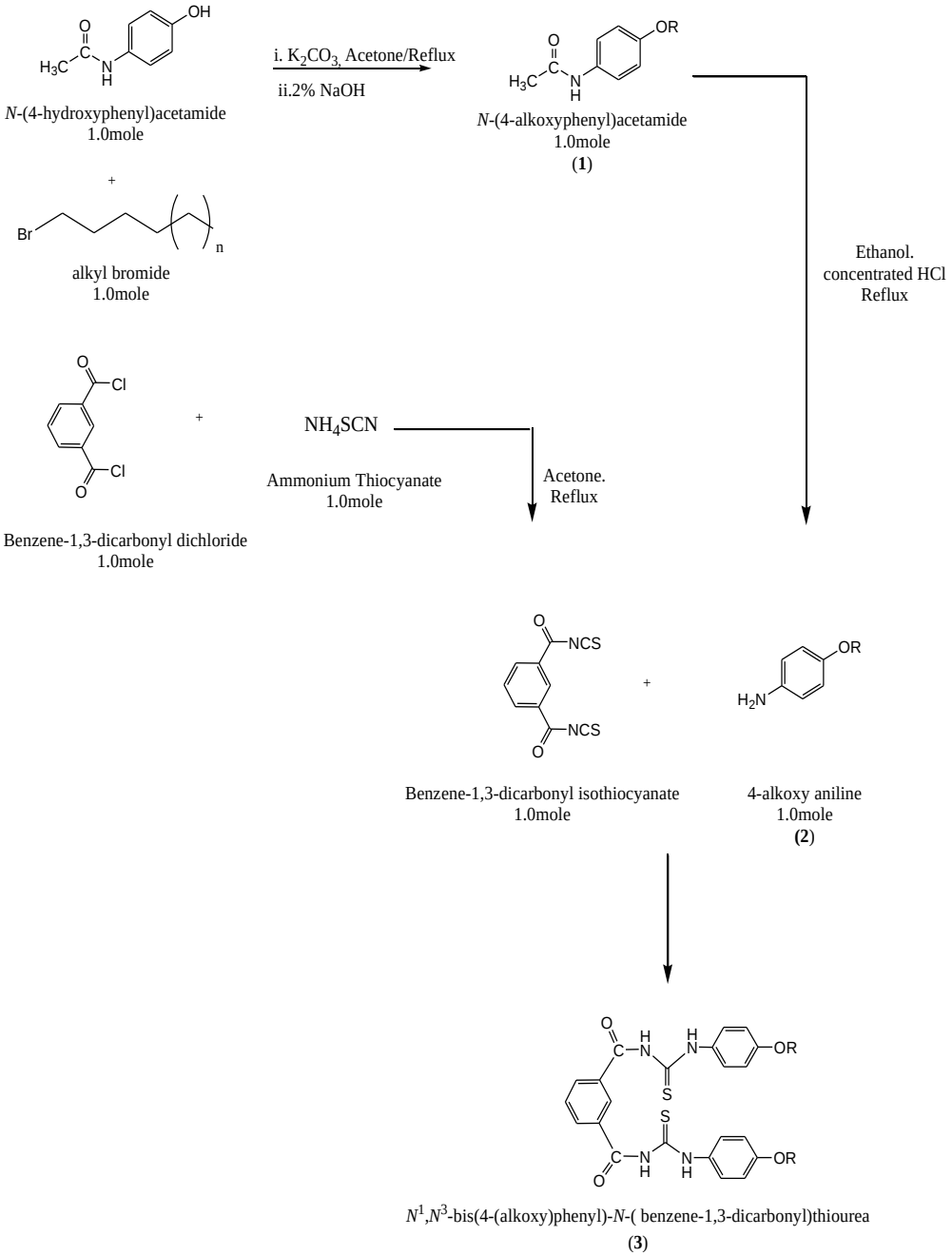

Scheme 1. General outline of synthetic work.

All chemicals or reagents used were purchased from standard commercial suppliers (Fisher Scientific, Merck and Sigma Aldrich) and used as received without further purification. All reactions were carried out under an ambient atmosphere and no special procedures were taken to exclude air or moisture during work-up. The infrared (IR) spectra were recorded on a Fourier Transform-Infrared

Spectrometer, Perkin Elmer Spectrum 100 in the range of 4000-400 cm^{-1} using potassium bromide (KBr) pellets. Meanwhile, for UV-Vis analysis, all compounds were recorded by using Spectrophotometer Shimadzu UV-1601PC in $1cm^3$ cuvette in methanolic solution for absorbance analysis. NMR spectra of ^1H and ^{13}C NMR were recorded using Bruker Avance III 400 spectrometer with deuterated chloroform ($CDCl_3$) as a solvent and chemical shift values were given in parts per million (ppm) relative to solvent resonances as internal standard. For CHNS elemental analysis was carried out by CHNS-O Analyzer Flashea 1112 series. The thermogravimetric analysis was performed using Perkin–Elmer TGA Analyzer from 0–700 °C at a heating rate of 10 °C/min under nitrogen atmosphere. Afterwards, the surface morphology of the final synthesized compounds in the form of powder and thin film were scanned by JSM 6360 Joel Scanning Electron Microscopy (SEM) with accelerated voltage 20 kV and magnification from 2000× until 10000×. The electrochemical study was performed using Electrochemical Impedance Spectroscopy (EIS) PGSTAT302 and electrical conductivity of the thin film was measured in the dark and under various light conditions by using Four-Point Probe and LI-200 Pyranometer Sensor with LI-1400 Data Logger while Keithley 4200 SCS Semiconductor Characterization System and Probe Station were used for efficiency determination.

2.2. Synthesis of N-(alkoxy)phenyl-N'-(benzene-1,3-dicarbonyl) thiourea

The synthesis of N^1,N^3-bis(4-(octyloxy)phenyl)-*N*'-(benzene-1,3-dicarbonyl) thiourea (**3**) derivative involved several continuous reaction which are *N*-(4-(alkoxy)phenyl) acetamide (**1**) as precursor, and 4-alkoxy aniline (**2**) as intermediate compound. For compound **1** and **2**, they have been reported before in previous occasions [18-21]. However, some modifications in synthetic work and further characterization on the spectroscopic and analytical tasks carried out are discussed further in this report. The synthetic pathway is described in Scheme 1.

*2.2.1 Preparation of N-(4-(octyloxy)phenyl) acetamide (**1**)*

The preparation of *N*-(4-(octyloxy)phenyl) acetamide was accomplished via synthesis through equimolar amount of *N*-(4-hydroxyphenyl) acetamide (10g, 66.2 mmol), octyl bromide (11.48 ml, 66.2mmol) and potassium carbonate (9.14g, 66.2 mmol). The mixture was put at reflux with constant stirring in *ca.* 100 ml acetone for *ca*. 48 hours to give white precipitate with colourless solution. When adjudged completion by TLC (Hexane: ethyl acetate) (2:3), the reaction mixture was cooled to room temperature before the solvent was taken to dryness to give white solid. The white solid obtained was then put at reflux with 2% of sodium hydroxide for *ca*. 1 hour to afford compound **1**.

*2.2.2. Preparation of 4-octyloxy aniline (**2**)*

The white solid of compound **1** (10.80g, 66.2 mmol) was put at reflux in ethanol (50ml) and concentrated hydrochloric acid (50ml) for *ca*. 2 hours to give a brown solution of 4-octyloxy aniline hydrochloride. The solution was then cooled at room temperature before extraction of the organic layer

from water: CH_2Cl_2 (150ml:150ml) was carried out. Organic layer was then separated and dried over $CaCl_2$ and solvent was removed *in vacuo* to give cream colour solid of the title compound, **2**.

*2.2.3. Preparation of N-(octyloxy)phenyl-N'-(benzene-1,3-dicarbonyl) thiourea (**3**)*

The synthesis of thiourea derivative involved a reaction between benzene-1,3-dicarbonyl dichloride (0.34 g, 1.0 mole) and ammonium thiocyanate (0.78g, 1.0 mole) which produced yellow solution after stirred in 50ml acetone for *ca*. 4 hours. Then, **2** (1g, 1.0 mole) was added to yellow solution and was put at reflux in acetone for *ca.* 4 hours. The progress of the reaction was monitored by using TLC in the solvent system hexane: CH_2Cl_2 (2:3). When adjudged completion, the mixture was filtered and the filtrate was left to cool at room temperature. The yellow filtrate was added with 3 ice cubes and filtered to obtain yellow precipitate. The yellow precipitate was then recrystallized from hot methanol to afford the title compound **3**. The physical properties with analytical data for compound **3** are shown in Table 1.

Table 1. Physical properties and analytical data of compound **3.**

Molecular formula of compound (3)	Products colour and Physical Property	Yield (%)	Percentage of weight Element			
			%C	%H	%N	%S
$C_{38}H_{50}N_4O_4S_2$	Pale yellow solid	65	66.02(66.05)	7.03 (7.29)	9.03 (8.11)	9.60 (9.28)

* In bracket: theoretical percentage of element

2.3 Electrochemical Measurements and Fabrication of Thiourea thin film on ITO Substrate

To assess intrinsic potential of compound **3** as active layer material, electrochemical properties was investigated using cyclic voltammetry via Electrochemical Impedance Spectroscopy (EIS) PGSTAT302. For this purpose, a conventional three-electrode cell was used with a platinum electrode. The platinum wire was used as counter electrode, Pt electrode as working electrode and Ag/AgCl electrode as reference electrode. In turn, **3** was deposited on the ITO substrate by using electrochemistry method in the following conditions: 0.05V, 0.05 V/S, potential range: -0.5V until 3.5V in acetonitrile and 0.5M sulphuric acid (as supporting electrolyte) with concentration of **3** ($1x10^{-3}$M).

Besides that, thin films were prepared by different techniques for each layer. First layer had been deposited on the ITO substrate was compound **3** by using electrochemistry method and second layer is chlorophyll (CHLO) thin film which was deposited on the top layer of compound **3**. ITO/**3** thin film was deposited by electrochemistry method by using Electrochemical Impedance Spectroscopy (EIS) PGSTAT 302. In turn, CHLO thin film was prepared by using the spin coating technique via

Spin Coater Model WS-400B-6NPP-LITE. Figure 2 shows the general illustration of layer arrangement in thin film.

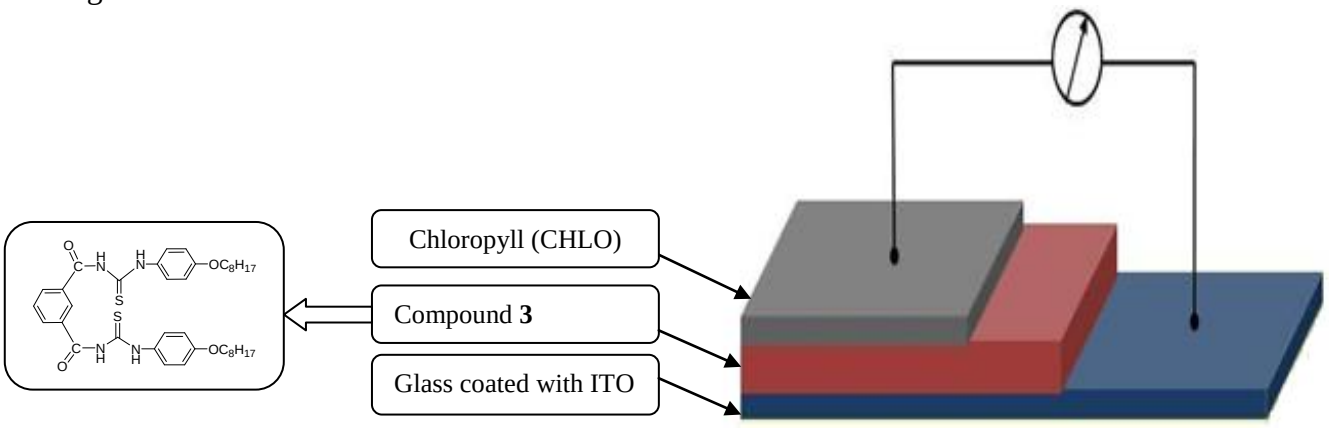

Figure 2. The general illustration of arrangement layer thin film

2.4 Electrical Conductivity of Thin Film under Various Intensity of Light

For electrical conductivity characterization, Four Point Probe system is used to determine the conductivity of **3** in form of thin film. In this study, the sheet resistivity in produced films was measured by using four point probing system consists of the Jandel Universal Probe combined with a Jandel RM3 Test Unit.

The electrical conductivity of thin film with different thickness was measured in the dark and light condition with intensity of 10 Wm^{-2}, 30 Wm^{-2}, 50 Wm^{-2}, and 100 Wm^{-2} respectively by using Four Point Probe and LI-200 Pyranometer Sensor with LI-1400 Data Logger. Current output, which is directly proportional to solar radiation, was calibrated against Eppley Precision Spectral Pyranometer (PSP) under natural daylight conditions in units of watts per square meter (Wm^{-2}). Under most conditions of natural daylight, the error is < 5 %. LI-1400 is a multipurpose data logger that functions both as a data logging device and a multichannel auto ranging meter.

3. RESULT AND DISCUSSIONS

3.1 Spectroscopic Studies

3.1.1. IR spectroscopy Analysis

The infrared spectra for **1-3** show six absorption bands of interest namely ν(N-H), ν(C-H), ν(C=O), ν(C-N), ν(C-O) and ν(C=S) which ranging from weak, moderate and strong intensities. Based on the IR spectrum of **1**, the absorption band for ν(C=O) was assigned at 1659cm^{-1} due to resonance of the lone pair of electrons on nitrogen to the C=O bond which almost identical in previous report with the similar systems [22-24]. Whilst, there is elimination of C=O amide functional group for the formation of compound **2** [25]. For spectra **2**, it shows broad strong absorption of N-H stretch at

3429cm^{-1} due to the intra-molecular hydrogen bonds [26,27]. The C-H alkane stretching, strong sharp absorption bands of C-N and C-O for these compounds are observed at 2922cm^{-1}, 1291cm^{-1} and 1170cm^{-1} respectively. Meanwhile, the IR spectrum for **3** revealed that there are two major existence for absorption band of interest namely C=O and C=S. The absorption bands for C=S in these compounds are observed at 748 cm^{-1} to 681 cm^{-1} as previously observed and reported at previous occasion [28, 29]. The absorption bands for C=S stretching have been assigned considerably at lower frequencies than the C=O vibration, in the C-N region, due to the greater mass of sulphur [29]. Therefore, the existence of new absorption bands of C=S proves that **3** is indeed a thiourea compound [30,31].

3.1.2 UV-Visible Spectroscopy Analysis

The electronic transitions of **1-3** were recorded in methanol as solvent in 1cm^{-3} cuvette with the wavelength ranges from 200-400nm. There are two major absorption bands of **1** which are C=O and Ar-O-R. The absorption band of C=O can be observed in range of λ_{max} 260 to 265nm respectively due to the formation of the hydrogen bond which increases the bond length of C=O. Smaller energy is required for this transition to take place and the absorption shows at the red end of the spectrum [32].

Meanwhile, the absorption of Ar-O-R is observed around λ_{max} 320 to 325nm which show transitions of $\pi\rightarrow\pi^*$ and $n\rightarrow\pi^*$ which are believed to be attributed to the phenyl ring in the molecules [33]. Whilst, the electronic transition of **2** shows two major bands which are expected to be contributed from Ar-NH_2 and Ar-O-R. The absorption bands for (-NH_2) and (-OR) chromophores are in range of 240 nm to 245 nm and 270 nm to 275 nm respectively because it exhibits two transition bands which are $\pi\rightarrow\pi^*$ and $n\rightarrow\pi^*$ for the functional group of phenyl ring and the substituent of the phenyl ring [34]. The substitution on the benzene ring can cause bathochromic or hyperchromic shift depends on the effect of electron donor or acceptor groups [35]. The substituents of alkoxy group and amine group act as the electron donating group on the aromatic ring constructed the bathochromic shift and shifted to longer wavelength. For **3**, it shows the elimination of Ar-NH_2 and existence of new absorption band of C=O and C=S on the range of λ_{max} 245nm and 275nm respectively. Normally, the thiol group will absorb at the range between 200 to 220 nm. However, in this study, due to the effect of π-conjugation of carbonyl group with the phenyl group, the transition of $\pi\rightarrow\pi^*$ and $n\rightarrow\pi^*$ shifted to the longer wavelength [36].

3.1.3 ^{1}H and ^{13}C Nuclear Magnetic Resonance (NMR)

The ^{1}H NMR spectra for compounds **1-3** show methyl resonance of alkoxy group in the range of δ_H 0.89-0.91 ppm while proton for the alkoxy group can be observed in the range of δ_H 1.31- 3.96 ppm. For R-O-CH_2, the signals of proton are detected in range of δ_H 3.88 – 4.00 ppm as singlet resonance because the protons on carbon attached to the oxygen are deshielded due to high electronegativity of the oxygen [37]. Whilst, aromatics proton are observed at around δ_H 6.64 – 7.62 ppm which show pseudo-doublet system and the resonance was strongly affected by *para*-substitution

on phenyl ring [38]. The resonances for aromatic ring are observed as multiplet resonances between δ_H 7.31-8.16 ppm which due to *o*, *m* and *p*-substituent methyl groups at the phenyl ring and overlapping of proton signals in the aromatic rings. Protons for N-H are observed as two singlet resonances due to presence of NH and NH_2 groups in these compounds which can be observed at δ_H 10.22 ppm and δ_H 11.56 ppm respectively. The complete ^{1}H NMR data for all synthesized compounds obtained (**1-3**) are tabulated in Table 2.

Table 2. ^{1}H NMR data of all the synthesized compounds (**1-3**).

Compound	Moieties	Chemical shift δ_H (ppm)
1	(t, $^3J_{HH}$ = 7 Hz, 3H, CH_3)	0.89
	(s, 3H, CH_3)	0.91
	(m, 12H, 6 x CH_2)	1.31-2.12
	(s, 2H, OCH_2)	3.90- 3.93
	(pseudo-d, $^3J_{HH}$ = 9Hz, 2H, C_6H_4)	6.84
	(pseudo-d, $^3J_{HH}$ = 9Hz, 2H, C_6H_4)	7.39
	(s, 1H, NH)	8.00
2	(t, $^3J_{HH}$ = 7 Hz, 3H, CH_3)	0.89
	(m,12H, 6 x CH_2)	1.32-2.20
	(s, 2H, OCH_2)	3.88-3.92
	(pseudo-d, $^3J_{HH}$ = 9Hz, 2H, C_6H_4)	6.64
	(pseudo-d, $^3J_{HH}$ = 9Hz,2H, C_6H_4)	7.28
	(s, 2H,NH_2)	10.04
] **3**	(t,$^3J_{HH}$=7Hz, 3H, CH_3)	0.84
	(m, 24H, 12H x CH_2)	1.25-2.50
	(s, 2H, OCH_2)	3.95-4.00
	(pseudo-d, 4H, 2 x C_6H_4)	6.92-6.95
	(pseudo-d, 4H,2 x C_6H_4)	7.52-7.62
	(2xs,1H, NH)	10.22-11.56

The ^{13}C NMR reveals the methyl (CH_3) and R–CH_2-O of alkoxy group can be detected in each synthesized compound (**1-3**). The resonance of this group can be observed in the range of δ_C 14.10-14.12 ppm. While the chemical shift for R–CH_2-O- of all compounds presence around δ_C 68.17-68.30 ppm due to deshielding effect in presence of oxygen atom that withdraws certain amount of electron from the alkyl chain [39]. Meanwhile, resonances of aromatic ring can be found in the range of δ_C 114.57 -130.97 ppm and the carbon for C=S and C=O are observed as singlet in the range of δ_C 155.88 ppm and 169.53 ppm respectively. The signal for carbonyl and thione carbons are slightly deshielded and can be observed in the range of δ_C 168.7-180.2 ppm in the spectra [40]. Resonances for C=O and C=S are slightly deshielded to higher chemical shifts may be due to formation of intra-molecular hydrogen bonding of the compounds and the increasing electronegativity of oxygen and

sulphur as well as different environment and conformation of oxygen and sulphur [38-41]. The ^{13}C NMR data for all compounds are shown in Table 3.

Table 3. The ^{13}C NMR data for all compounds (**1-3**)

Compound	Moieties	Chemical shift δ_C (ppm)
1	(CH_3-for alkoxy) (CH_3-for methyl) (6xCH_2) (CH_2-O) (C_6H_4) (C=O)	14.10 22.66 24.1-31.82 68.31 114.70-155.99 169.71
2	(CH_3) (6xCH_2) (CH_2-O) (C_6H_4)	14.10 22.68-31.87 68.17 115.17-158.93
3	(CH_3) (6xCH_2) (CH_2-O) (C_6H_4) (C=O) (C=S)	14.11 22.68-31.88 68.23-68.29 114.57-130.97 155.88 169.53

3.2. Thermal Stability Analysis

3.2.1. Thermogravimetric Analysis (TGA)

Thermal stability of the material is crucial to be investigated for fabrication of thin film which in turn, will be applied onto the solar cell for photovoltaic application [42]. Long term stability for the material will increase the stability of the thin film of solar cell under high temperature environment over long period of time. Therefore, the thermal properties of all compounds (**1-3**) were investigated by TGA at heating rate 10°C/min under nitrogen atmosphere with temperature range of 30 – 800 °C. The result of thermograms is presented in Figure 3.

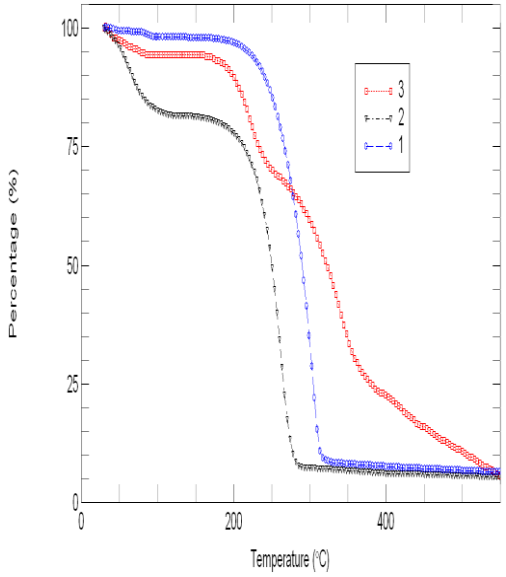

Figure 3. TGA thermograms of all synthesized compounds (**1-3**).

From the thermograms as illustrated in Figure 3, it shows **1** has the highest onset temperature in the range of 230-240°C while **2** starts to degrade at 120°C. Meanwhile, temperature of onset **3** shows two stages of major weight loss at 238°C and 310°C. From the thermogram, there is no weight loss occurs below 100°C which show that there is no water molecule or solvent in the sample [43]. The temperature of **1** is higher than **2** due to reason that it has higher molecular weight and bulky compounds. Whilst, it has found that the onset temperature of **3** was higher than **2** and it could be explained in term of the conjugated compound of thiourea and overlapping orbitals between C=S and C=O. Besides, the thermal stability of compound was increased as the temperature of degradation increases and it depends on the number of aliphatic carbon chain [44]. Therefore, it can be summarized that **1** is thermally stable according on its onset temperature, however **3** shows the most stable compound among its precursors due to it has taken the longest time to complete the degradation process. Thus, all synthesized compounds show good potential of thermal stability under high temperature and it is proven these compounds can behave great potential coating material for the fabrication of solar cells [45].

3.3. Surface Morphology

3.3.1 Scanning Electron Microcopy (SEM) Analysis

Scanning Electron Microscopy analysis was utilized in order to analyze the surface morphology of thiourea compound in powder form and on the ITO substrate in term of distribution of sample in thin film fabrication. Figure 4 shows the surface morphology obtained for **3** as a focalpoint compound in this study in powder form. Whilst, Figure 5 depicts the image of **3** on the ITO substrate.

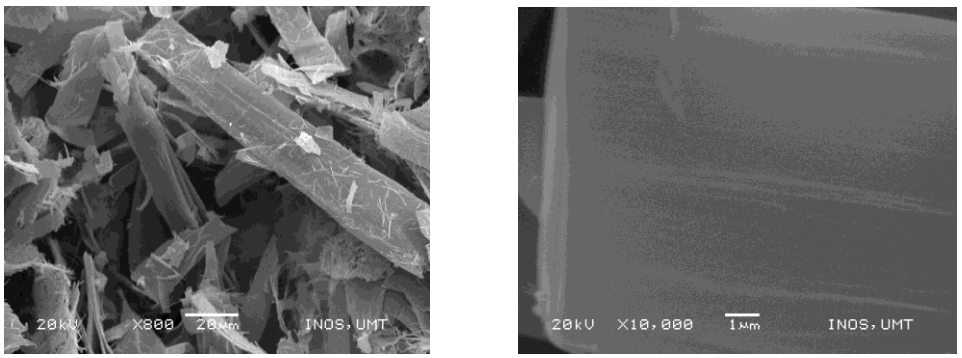

(a) (b)

Figure 4. Surface morphology of compound **3** at (a) (x800 magnification) (b) (x10000 magnification)

From the micrograph, the image of **3** exhibits as board-like, compact, smooth and branches surface as shown in Figure 4. The surface morphology of **3** shows good crystanility which could promise smooth distribution on ITO surface during thin film fabrication. In addition, the smoothness distribution on ITO substrate enhances the efficient absorption of sun energy to give high electrical conductivity and thus, enhance its performance as organic solar cell.

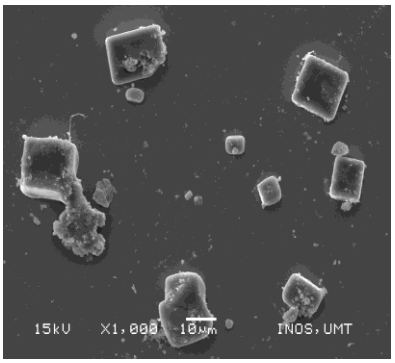

Figure 5. Surface morphology of compound 3 on ITO substrate.

In turn, the image of **3** on ITO substrate also was scanned and viewed as shown in Figure 5. **3** was coated on ITO substrate by using electrochemistry method in specific conditions and parameters. Electrodeposition method is one of the useful and simple methods compared to others which bring few benefits such as low cost, minor waste of material and have ability to deposit on thin film with a complex surface [46,47]. Based on the SEM image, **3**/ITO exhibits cube shaped, smooth and solid surface which quite similar with their image in the powder form. However, obviously it can be seen that the length and area structures of **3** formed on ITO surface differ with the powder image of **3** due to the process of both final compounds went through during electrochemical deposition. Thus, from SEM images, it can be concluded that **3** could be able to form a compact layer on ITO and improve the adhesion of the absorber layer to the ITO.

3.4 Electrochemistry Study

3.4.1 Cyclic Voltammetry Analysis

The electrochemical behaviour of **3** was investigated further by using cyclic voltammetry in order to determine the potential range of different electrochemical processes [48]. The initial electrochemical study 1×10 M^{-3} of **3** in acetonitrile has been studied which is shown in Figure 6. From the voltammograms curves, it clearly shows that there is no redox peaks in this electrochemistry process, thus it can be said that the electro-oxidation of **3** on platinum did not occur in the solvent individually. This is because **3** is a fairly large polarizable molecule which is most likely to be solvated poorly in aqueous solutions to exhibit acid-base properties [49]. Meanwhile, in aqueous solution, **3** decomposes slowly at room temperature but only limited information about the stability of these solutions in different environments are available [18].

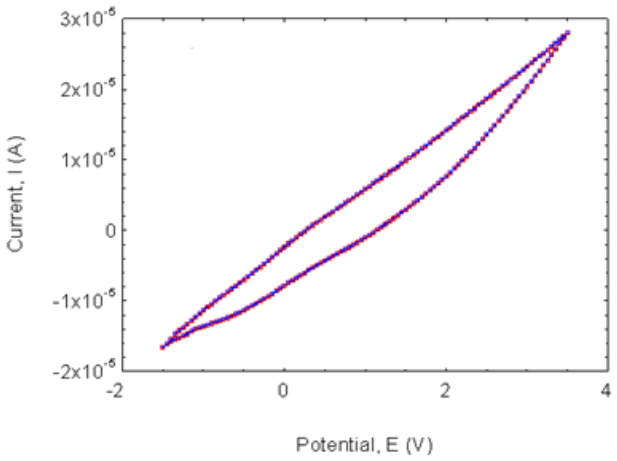

Figure 6. Cyclic Voltammogram of 3 in CH_3CN on Pt electrode.

However, when using 0.5 M sulphuric acid as supporting electrolytes, the cyclic voltammogram of **3** reveals a redox reaction. The oxidation peak occurs at ΔEpa= 0.55V with Ipa= $1x10^{-4}$ A and ΔEpa= 1.43V with Ipa= $4.03x10^{-4}$ A while the reduction peak occurs at ΔEpc= 1.2V with Ipc=$0.52x10^{-4}$A and ΔEpc= 0.30V with Ipc= $-2.56x10^{-4}$A, as shown in Figure 7. Therefore, it can be concluded that the peak becomes better defined when the potential scan goes from 0 to 1.6V. Obviously, the electrochemistry of **3** appears in the positive region with its electro-oxidation stage, peak B and peak A as a cathodic peak with a peak to peak separation is about 1 V.

It has been reported that formamidine disulphide (FDS) ions are formed as a product from thiourea (TU) electro-oxidation in acidic solutions on platinum, by either chemical or electrochemical methods [50]. In addition, Jiang and co-workers claimed that FDS is one of the products of TU oxidation path on platinum in the presence of chloride ions using cyclic voltammetry. There was a report claimed that the first oxidation TU is defined around 0.7 V which represents to the formation of formamidine disulphide (FDS) [51]. From the cyclic voltammagrams, formamide disulphide ion is formed as a product when **3** oxidizes on platinum in acidic solution with the presence of chloride ion

analysed by electrochemical methods. This is may be due to sulphur is absorbed on platinum surface which could be further oxidizes into HSO^{-4} and SO_4^{-2}. From this study, it can be concluded the stage of the electro-oxidation stages occurred around 1.2V in order to claim the formation of FDS.

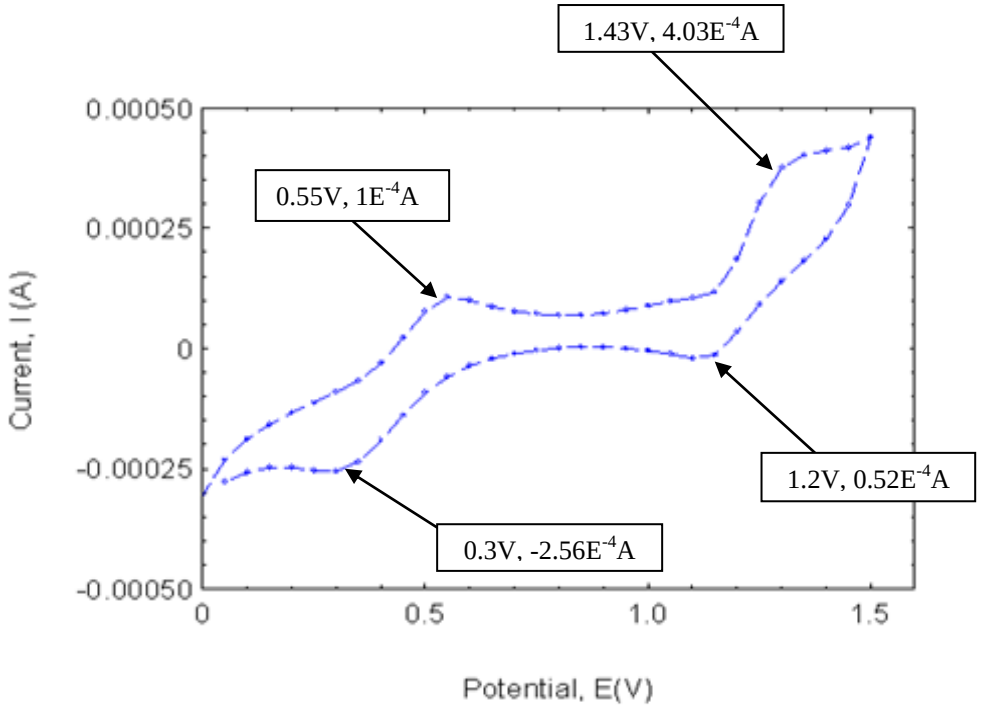

Figure 7. Cyclic voltammogram of **3** ($1x10^{-3}$M) in CH_3CN + 0.5M sulphuric acid run at 0.03V, $0.03Vs^{-1}$

3.5 Electrical Conductivity of Thin Film in Dark and under Intensity of Light

The electrical conductivity (EC) study of **3**/ITO and CHLO/**3**/ITO thin films were measured and compared under various light and intensities by using Four Point Probe. The electrical conductivity is shown in Table 4 and bar chart of electrical conductivity measurements data in Figure 8 is obtained from these values.

Table 4. The electrical conductivity of **3**/ITO and CHLO/**3**/ITO in following conditions

Intensity (Wm^{-2})	Electrical Conductivity σ (Scm^{-1})	
	Without CHLO	With CHLO
Dark condition	0.1297	0.1314
Light Condition ($10Wm^{-2}$)	0.1306	0.1330
Light Condition ($30Wm^{-2}$)	0.1334	0.1345
Light Condition ($50Wm^{-2}$)	0.1350	0.1362
Light Condition ($100Wm^{-2}$)	0.1370	0.1377

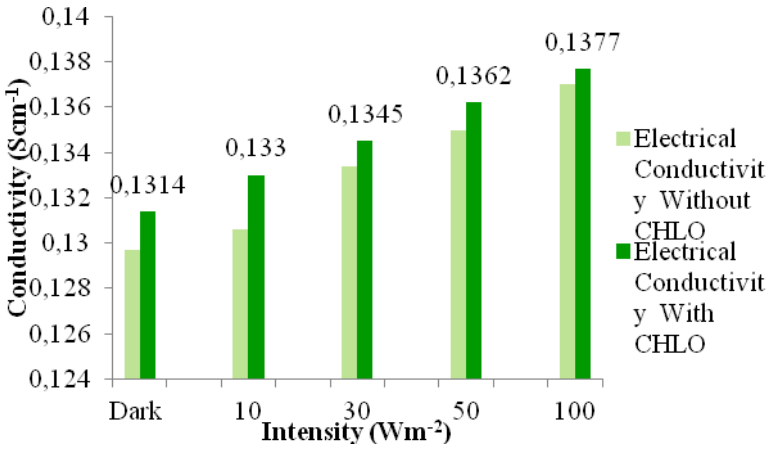

Figure 8. The electrical conductivity of **3**/ITO and CHLO/**3**/ITO

From the data analysis, it is obvious to clarify that **3** can conduct electricity even in dark conditions. Hence, it is clearly shown **3** can conduct electricity without obtaining energy from the sunlight. Besides, Figure 8 shows their electrical conductivity increases by the increasing light intensities. From the graph, the highest conductivity is observed under maximum light intensity ($100Wm^{-2}$) with the conductivity value of 0.1370 Scm^{-1}. From the results obtained, it is clearly shows that with the increasing of the light intensity have given highest electrical conductivity of the **3**/ITO thin film.

As expected, with the presence of chlorophyll (CHLO) will increase the performance of organic solar cells. When chlorophyll layer combined with thin film of **3** to form CHLO/**3**/ITO, it shows the electrical conductivity increased in the same conditions. It shows the conductivity of 0.1377 Scm^{-1} under maximum light intensity. The electrical conductivity under influence of intensity of light increases with the increasing values and the positive result obtained showed that the thin films were successfully coated on the ITO substrate. Thus, it can be concluded **3** has great potential and promising conducting material and as active layer in organic solar cell.

4. CONCLUSIONS

Novel V-shaped conjugated organic compound namely N^1,N^3-bis(4-(octyloxy)phenyl)-*N*'-(benzene-1,3-dicarbonyl) thiourea were successfully synthesized, characterized and investigated as an active layer for application in organic solar cell. All synthesized compounds including the precursors and final product were characterized via typical spectroscopic and analytical methods for their physical, structural, thermal and also electrical properties by CHNS, IR, UV-Vis, ^1H and ^{13}C NMR, TGA, SEM, CV, and Four Point Probe for its electric conductivity behaviour. From the electrical conductivity study, it revealed the layer of Chlorophyll (CHLO)/**3**/ITO thin film exhibits higher conductivity, $0.1377Scm^{-1}$ compared to the layer of **3**/ITO thin film without CHLO, $0.137Scm^{-1}$ under maximum light intensity ($100Wm^{-2}$). From the results of spectroscopic and analytical analysis, it is proven the **3** was successfully synthesized due to good agreement with the proposed molecular

structure and proved its potential in OSC. Therefore, these findings provide the following insights for future study which brings new prospective in molecular device application.

ACKNOWLEDGEMENT
Special acknowledgement is dedicated to Ministry of Higher Education, Malaysia (MOHE) for the funding of this research (FRGS59253), Advanced Materials Research Group, Department of Chemical Sciences and Department of Physical Sciences, Faculty of Science and Technology for research facilities, Institute of Marine Biotechnology (IMB) and Institute of Oceanography (INOS) for NMR and SEM analysis respectively.

References

1. D. A. Lashof, D. R. Ahuja, *Relative Contributions of greenhouse gas emission to global warming*., 34 (1990) 529-531.
2. J. K. Casper, Energy powering the past, present and future, Chelsea House Publishers, New York, 2007.
3. S. O. Kang, D. Kim, M. S. Kang, K. Song and J. Ko, *Tetrahedron.*, 64 (2008) 10417-10424.
4. K. Zweibel, *Solar Energy Materials and Solar Cells.*, 63 (2000) 375-386.
5. M. Grätzel, *Philosophical Transactions of the Royal Society.*, 365 (2007) 993-1005.
6. C. J. Brabec, (2004). *Solar Energy Materials and Solar Cells.*, 83 (2004) 273 – 292.
7. K. L. Chopra, P. D. Paulson, and V. Dutta, *Thin-film Solar Cells: An Overview*., 12 (2004) 69-92.
8. H. Mizuseki, N. Igarashi, C. Majumder, R. V. Belosludov, A. A. Farajian and Y. Kawazoe, *Thin Solid Films.*, 438 (2003) 235 – 237.
9. J. Nelson, *Solid state & material science.*, 6 (2002) 87-95.
10. X. Yin, Y. Li, Y. Zhang, P. Li and J. Zhao, *J. Chem. Phys Lett.*, 422 (2006) 111 - 116.
11. J. Zhao, Y. Li, and G. Yin, *Computational Material Science.*, 39 (2007) 775-781.
12. K. Sanghoon, C. Hyunbong, B. Chul, S. Kihyung, O. K. Sang and K. Jaejung., *Tetrahedron* 63 (2007) 11436 – 11443.
13. M. G. Kang, H. J. Park, S. H. Ahn, T. Xu, and L. J. Guo, *Toward Low-Cost, High-Efficiency, and Scalable Organic Solar Cells with Transparent Metal Electrode and Improved Domain Morphology*. IEEE Journal of Selected Topics In Quantum Electronics. (2010)
14. J. Zhao, Y. Li, and G. Yin, *Computational Material Science.*, 39 (2007) 775-781.
15. S. H. Baek, H. S. Jang and H. K. Kim, *Curr. Appl. Phys.*, 11 (2010) 30-33.
16. A. Goetzberger, C. Hebling, and H. Schlock, *Materials science and engineering.*, 40 (2003) 1-46.
17. D. Goldhaber-Gordon, M. S. Montermerlo, J. C. Love, G. J. Opiteck, and J. C. Ellenbogen, *Overview of Nanoelectronic Devices. Proceedings of the IEEE, Nanoelectronics,* (1997).
18. H. K. Adli, W. M. Khairul, H. Salleh, *Int. J. Electrochem.*, 7 (2012) 499-515.
19. D. Rais, Y. Zakrevskyy, J. Stumpe, S. Němpůrek, and Sedláková. *Optical materials.*, 30 (2008) 1335-1342.
20. M. Chao-Mei, M. Kully, J. K. Khan, M. Hattori and Daneshtabb. *Bioorganic and Medical Chemistry.*, 15 (2007) 6870-6833.
21. E. Westphal, I. H. Bechtold and H. Gallardo, *Macromolecules.*, 43 (2010) 1319-1328.
22. M. Kukut, B. Kiskan and Y. Yangci, (2009). *Des. Mon. Polym.*, 12 (2009) 167-176.
23. G. Kavak, S. özbey, G. Bİnzet and N. KÜlcÜ, (2009). *Turk. J. Chem.*, 33(2009) 857 – 868.
24. M. Mureseanu, A. Reiss, N. Cioatera, I. Trandafir, I. and V. Hulea, *J. Hazard. Mat.*, 182 (2010) 197 – 203.
25. Y. Akiyama, S. Fujita, H. Senboku, C. M. Rayner, S. A. Brough and M. Arai, *J. Supercrit. Fluids*.,46 (2008) 197 - 205.

26. A. Y. Arasi, J. J. L. Jeyakumari, B. Sundaresan, V. Dhanalakshmi and R. Anbarasan, *Spectrochim. Acta Part A.*, 74 (2009) 1229 - 1234.
27. D. Gambino, E. Kremer, and E. J. Baran, *Spectrochim Acta Part A.*, 58 (2002) 3085 - 3092.
28. O. Estévez-Hernández, E. Otazo-Sánchez, J. L. H. H. de Cisneros, I. Naranjo-Rodríguez and E. Reguera, *Spectrochim Acta Part A.*, 62 (2005) 964-971.
29. R. Kakkar, A. Dua and S. Zaidi, *Spectrochimica Acta Part A.*, 68 (2007) 1362-1369.
30. P. Bombicz, I. Mutikainen, M. Krunks, T. Leskelá, J. Madarász and Niinistö. *Inorganica Chimica Acta.*, 357 (2004) 513 – 525.
31. J. T. J. Prakash, L. R. Nirmala, *International Journal of Computer Applications*., 6 (2010) 0975 – 8887.
32. G. Madhurambal, M. Mariappan and S. C. Mojumdar, *J. Therm. Anal. and Calorim*., 100 (2010) 853 – 856.
33. D. L. Pavia, G. M. Lampman and G. S Kriz, *Introduction to Spectroscopy. 3rd Edition*. Thomson Learning Inc. 2001.
34. C. A. Cutler, A. K. Burrell, D. L. Officer, C. O. Too and G.G. Wallace, *Synthetic Metals*., 128 (2001) 35–42.
35. M. M. M. Raposo, G. Kirsch, *Tetrahedron., (*59) (2003) 4891-4899.
36. H. K. Adli, W. M. Khairul and H. Salleh, (2011*). International Journal of Advanced Chemical Technology*. 1 (2011) 01-05
37. M. S. M. Yusof, N. A. Mushtari and B. M. Yamin, *Acta Crystallographica Section E*., (2007) 1600-5368.
38. M. S. M. Yusof, R. H. Jusoh, W. M. Khairul and B. M. Yamin, *J. Mol. Struct*., 975 (2010) 280-284.
39. A. Tadjarodi, F, Adhami, Y. Hanifehpour, M. Yazdi, Z. Moghaddamfard and G. Kickelbick, *G. Polyhedron* 26 (2007) 4609 – 4618.
40. İ. Küçükgüzel, E. Tatar, S. G. Küçükgüzel, Ş. Rollas, S. and E. De Clercq, *European Journal of Medicinal Chemistry* (43) (2008) 381-392.
41. A. Saeed, U. Shaheen, A. Hameed, and S. Z. H. Naqvi, *Journal of Fluorine Chemistry.*, 130 (2009) 1028–1034.
42. M. M. M. Raposo, A. M. F. P. Ferreira, M. Belsley and J. C. V. P. Maura, *Tetrahedron.*, 64 (2008) 5878-5884.
43. H. H. Tønnensen., *International Journal of Pharmaceutical*., 1 (2010) 225.
44. B. J. Vasanthi, L. Ravikumar, *European Polymer Journal*., 43 (2007) 4325-4331.
45. T. A. Li, W. F. Chen, A. Cuevas and J. E. Cotte, (2007). *Thermal Stability of Microwave PECVD Hydrogenated Amorphous Silicon As Surface Passivation For N-type Heterojunction Solar Cells. European Photovoltaic Solar Energy Conference (WIP-Renewable Energies, Germany).*, (2007) 1326 – 1331.
46. T. P. Gujar, W. Y. Kim, I. Puspitasari, K. D. Jung and O. S. Joo, *Int. J. Electrochem.*, 2 (2007) 666 – 673.
47. L. Chen, S. Shet, H. Tang, H. Wang, T. Deutsch, Y. Yan, J. Turner and M. Al- Jassim, *Journal of Material Chemistry* 20 (2010) 6962 –6967.
48. M. Mouanga and P. Bercot, *Int. J. Electrochem*., 6 (2011) 1007-1013.
49. M. Hoffmann, J. O. Edwards, *Inorganic Chemistry* 16 (1977) 3333 – 3338.
50. A. E. Bolzán, I. B. Wakenge, R. C. Salvarezza and A. J. Arvia, *Journal of Electroanalytical Chemistry* 475 (1999) 181 – 189.
51. M. Yan, K. Liu and J. Z. Jiang, *Journal of Electroanalytical Chemistry*., 408 (1996) 225 – 229.